THE JOURNAL OF BIOLOGICAL CHEMISTRY VOL. 288, NO. 3, pp. 1829–1840, January 18, 2013

Monomeric Synucleins Generate Membrane Curvature*[S]

Received for publication, September 11, 2012, and in revised form, November 13, 2012 Published, JBC Papers in Press, November 26, 2012, DOI 10.1074/jbc.M112.418871

Christopher H. Westphal[‡§1] **and Sreeganga S. Chandra**[‡¶‖2]

From the [‡]*Program in Cellular Neuroscience, Neurodegeneration and Repair,* [§]*Department of Cell Biology,* [¶]*Department of Neurology, and* [‖]*Department of Molecular, Cell, and Developmental Biology, Yale University, New Haven, Connecticut 06536*

Background: α-Synuclein is a protein of unknown function that is critical for Parkinson disease pathology.
Results: All members of the synuclein family can bend membranes when monomeric.
Conclusion: Synucleins function at the presynaptic terminal to facilitate membrane curvature generation during synaptic vesicle exo- and endocytosis.
Significance: Elucidating synuclein function is important for understanding vesicle trafficking and synaptic dysfunction in Parkinson disease.

Synucleins are a family of presynaptic membrane binding proteins. α-Synuclein, the principal member of this family, is mutated in familial Parkinson disease. To gain insight into the molecular functions of synucleins, we performed an unbiased proteomic screen and identified synaptic protein changes in αβγ-synuclein knock-out brains. We observed increases in the levels of select membrane curvature sensing/generating proteins. One of the most prominent changes was for the N-BAR protein endophilin A1. Here we demonstrate that the levels of synucleins and endophilin A1 are reciprocally regulated and that they are functionally related. We show that all synucleins can robustly generate membrane curvature similar to endophilins. However, only monomeric but not tetrameric α-synuclein can bend membranes. Further, A30P α-synuclein, a Parkinson disease mutant that disrupts protein folding, is also deficient in this activity. This suggests that synucleins generate membrane curvature through the asymmetric insertion of their N-terminal amphipathic helix. Based on our findings, we propose to include synucleins in the class of amphipathic helix-containing proteins that sense and generate membrane curvature. These results advance our understanding of the physiological function of synucleins.

α-Synuclein is a key protein in the pathology of many neurodegenerative diseases, most notably Parkinson Disease (PD).[3] In this neurodegenerative disease, α-synuclein is the major component of the intracellular protein aggregates known as Lewy bodies (1). α-Synuclein is also genetically linked to PD. Three point mutations in the α-synuclein gene (*SNCA; PARK1*) and gene multiplications (*PARK4*) cause familial PD (2–4). Genome-wide association studies have revealed that sequence variants in *SNCA* are strongly associated with sporadic cases of PD (5, 6).

Although its involvement in neurodegenerative diseases is well established, the physiological function of α-synuclein is unknown. α-Synuclein is a member of a family of three presynaptic proteins that includes β- and γ-synuclein. Previous molecular studies have implicated synucleins in synaptic vesicle trafficking (7, 8). More recently, studies of synuclein knock-out mice have revealed that synucleins upregulate neurotransmission by influencing either synaptic vesicle exo- or endocytosis (9–12). Intriguingly, transgenic mice overexpressing wild type α-synuclein show decreased neurotransmission, opposite to the phenotype of synuclein knock-out mice (13, 14). This indicates that in case of *PARK4* patients, the normal synuclein function is being perturbed. Thus, understanding the precise molecular function of synucleins is important to gain further insight into regulation of the synaptic vesicle cycle as well as synaptic dysfunction in PD.

Structurally, synucleins are ~14 kDa proteins with highly conserved N termini and divergent C termini (supplemental Fig. S1*A*). The N terminus of synucleins contains 7 copies of an 11-residue imperfect *X*KTKEGV*XXXX* repeat similar to those seen in the amphipathic helices of class A2 apolipoproteins (supplemental Fig. S1*A*; Ref. 15). The C terminus is highly acidic and has many prolines. Synucleins are thought to be natively unfolded proteins in solution that adopt α-helical conformations when the monomeric protein binds lipid membranes. However, recently it was shown that α-synuclein also exists as an α-helical tetramer both in solution and on the membrane (16, 17).

All members of the synuclein family interact robustly with acidic lipid membranes (15, 18). Upon binding membranes, the N terminus of monomeric α-synuclein folds into one of two amphipathic α-helical conformations. This conformation can be either an uninterrupted N-terminal α-helix (~93 amino acids; Ref. 19) or two anti-parallel helices, *i.e.* a broken α-helix (break at amino acid 44–45; Ref. 18, 20). In both conformations there is partial insertion of the N-terminal hydrophobic residues into the outer leaflet of the membrane, while the C termi-

* This work was supported, in whole or in part, by grants from the National Institutes of Health (R01 NS064963), the Bumpus Foundation, and an Anonymous Foundation grant (to S. S. C.). The proteomics was done with the support of the Yale Keck NIDA Neuroproteomic Center (P30 DA018343).
[S] This article contains supplemental Figs. S1—S7.
[1] Supported in part by NIH Grant T32GM7223.
[2] To whom correspondence should be addressed: Program in Cellular Neuroscience, Neurodegeneration and Repair, Department of Neurology, and Department of Molecular, Cell and Developmental Biology, Yale University, 295 Congress Ave., New Haven, CT. Tel.: 203-785-6172; Fax: 203-737-1761; E-mail: sreeganga.chandra@yale.edu.
[3] The abbreviations used are: PD, Parkinson Disease; DIGE, two-dimensional fluorescence difference gel electrophoresis; iTRAQ, isobaric tag for relative and absolute quantitation; BPL, brain polar lipids; KO, knockout.

nus remains unfolded. The exact α-helical conformation adopted depends on the curvature of the membrane: the broken helix is formed on highly curved lipid surfaces, while the longer helix is formed on flatter lipid surfaces (21, 22). Thus, α-synuclein possesses the hallmarks of being a membrane curvature sensor. Congruently, α-synuclein preferentially binds to smaller lipid vesicles, *i.e.* those with higher membrane curvature (15). α-Synuclein affinity for lipid vesicles is increased dramatically at around 45 nm, the size of a synaptic vesicle (23). Indeed, α-synuclein has been localized to synaptic vesicles by immuno-electron microscopy (24). While the tetrameric form of α-synuclein also binds acidic lipid membranes (16), it is not known if binding is membrane curvature-dependent.

Recent *in vitro* experiments using synthetic lipid mixtures have revealed that synucleins can also generate membrane curvature (25–27). However, it is still unclear if synucleins can bend neuronal membranes, especially at concentrations likely to be present at synapses. Further, the ability of tetrameric α-synuclein to generate membrane curvature remains to be established. Importantly, it is not known if the membrane bending properties of synucleins are physiologically relevant. Therefore, we set out to biochemically characterize αβγ-synuclein KO mice and investigate the ability of synucleins to generate membrane curvature in a physiologically relevant setting. These studies shed interesting new light on the function of these presynaptic proteins.

EXPERIMENTAL PROCEDURES

Constructs and Antibodies—Human and mouse synuclein constructs have been described previously (18, 28) except for the human E46K α-synuclein expression construct, which was made by site-directed mutagenesis. Endophilin A1 bacterial expression construct was a kind gift of Dr. Pietro De Camilli, Yale University. α-Synuclein (BD Biosciences), Annexin A5 (Abcam), and actin (MP Biomedical) antibodies were purchased, while antibodies to endophilins and FCHO1 were a gift from Dr. Pietro De Camilli, Yale University.

Mice—αβγ-synuclein KO and the rescued mice have been described previously (12). All mice were housed at Yale University under an IACUC approved protocol.

Synaptosome Fractionation—Wild type and αβγ-synuclein KO brains were fractionated according to the protocol of Ref. 29.

Mass Spectrometry—A quantitative analysis of the synaptic proteome of wild type and αβγ-synuclein KO mice was performed using DIGE according to previously published protocols (30, 31). Equal amounts of protein from wild type and αβγ-synuclein KO samples were differentially labeled *in vitro* with Cy3 and Cy5 *N*-hydroxysuccinimidyl ester dyes and separated on two-dimensional gels. Differentially expressed protein spots were robotically excised and subjected to in-gel trypsinization. The peptides were analyzed on a matrix-assisted laser desorption/ionization time-of-flight spectrometer (MALDI ToF/ToF; Applied Biosystems model 4800). The resulting, uninterpreted MS/MS spectra were searched against the IPI mouse database 3.27 using Mascot algorithms to enable high-throughput protein identification.

Wild type and αβγ-synuclein KO samples were subjected to 4-plex iTRAQ with technical replicates as described (32). The samples were trypsin digested, labeled with iTRAQ tags, pooled, fractionated by cation exchange, and the individual peptides were run on an Applied Biosystems API Q-Star XL mass spectrometer. iTRAQ quantitation and protein identification were performed using the Paragon search algorithm (33) in ProteinPilot 2.0 software against the IPI mouse database.

Stringent criteria were used to identify changes in αβγ-synuclein KO samples. For the DIGE experiments, proteins that were identified by at least two independent peptides and whose levels were increased by at least 1.4-fold were considered. For the iTRAQ experiments, at least two independent peptides with valid iTRAQ reporter ion ratios, exhibiting a minimum of two iTRAQ reporter ions with a summed S/N ratio >9 were required to be included in the analysis. The cut-off for iTRAQ experiments was set to 1.2-fold. The proteins that met these criteria and were replicated in two technical and two biological replicates are listed in Fig. 1. The mass spectrometry data are publically available through the YPED Repository.

Recombinant Protein Purification—Monomeric, recombinant α-, β-, and γ-synuclein were purified as GST-fused constructs and cleaved using the TEV protease as described (18). Endophilin was purified from a GST-fused construct using the PreScission protease (GE Healthcare) as described (34). All proteins were dialyzed against 20 mM HEPES buffer, pH 7.4. Purified synaptobrevin 2 was a kind gift of Dr. Yongli Zhang, Yale University.

Preparation of Liposomes—Lipid mixtures composed of either 50% DOPE/40% DOPS/10% cholesterol (all lipids from Avanti Polar Lipids) or brain polar lipids (BPL; Avanti Polar Lipids) were prepared at 10 mg lipid/ml in chloroform. Rhodamine-labeled DHPE (Invitrogen) was added to 2% for fluorescent imaging as needed. The liposomes were made to a lipid concentration of 1 mg/ml following the protocol of Ref. 35. The average diameter of the liposomes was ~3 microns.

Purification and Characterization of α-Synuclein Tetramer from Human Blood—α-Synuclein tetramer was purified from 120 ml freshly drawn human blood as described in Ref. 16. Circular dichroism spectroscopy was done on an Applied Photophysics Chirascan CD Spectrometer with or without BPL liposomes at 1 mg/ml. Data were collected in a 0.1 cm cuvette at a temperature of 25 °C. Buffer and liposome spectra were subtracted from sample measurements, and the data are presented as mean residue ellipticities.

Fluorescence Tubulation Assay—2 μl of protein at the denoted concentrations and 2 μl of liposomes were mixed with 10 μl 20 mM HEPES buffer, incubated at 37 °C for 10 min, and then kept on ice until imaging. Membrane tubulation was imaged in a chamber as in Ref. 36. In all tubulation assays except in Fig. 5*A* and supplemental Fig. S7, the molar lipid/protein ratio was ~1000:1. In Fig. 5*A*, the molar lipid/protein ratio varied but was not less than 200:1, a ratio at which α-synuclein is still fully folded (18). In supplemental Fig. S7, the molar lipid/protein ratio was not less than 100:1. To quantify the tubule and lipid area, one picture was taken every second for 1 min, and the tubule area/total lipid area quantified for each image.

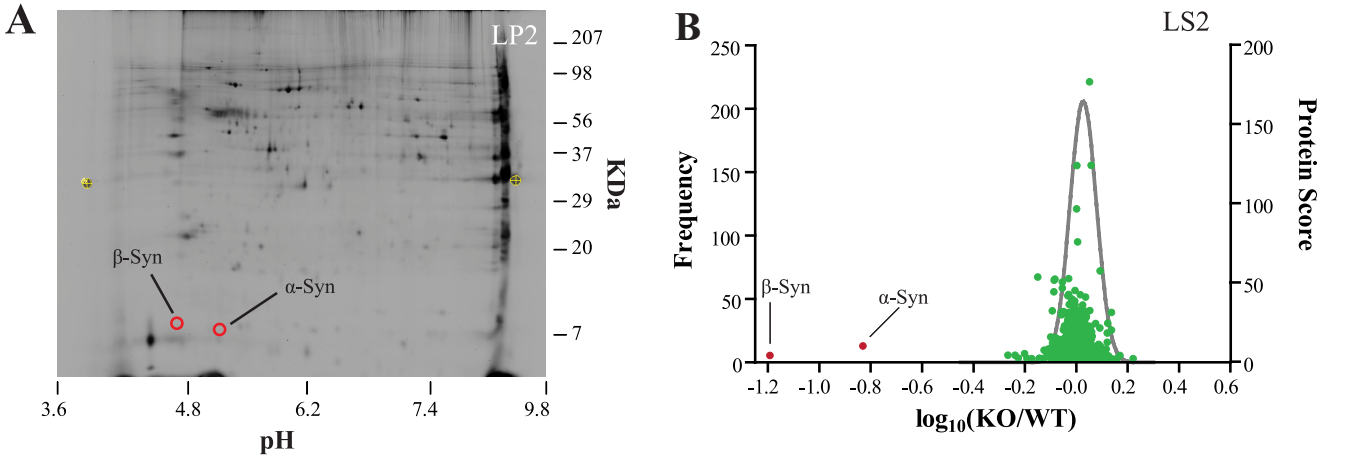

C

Protein Name	Fold Change	Peptides	Method	Validated	Lipid Binding	Function
Endophilin A1	1.53 ± 0.080 1.28 ± 0.013	12-17 13-14	DIGE iTRAQ	+	Yes	Endocytosis/ Membrane Curvature
Endophilin B2	1.26 ± 0.044	5-9	iTRAQ	+	Yes	Membrane Curvature
Synapsin IIb	1.79 ± 0.151	13	DIGE	+	Yes	Vesicle Trafficking/ Membrane Curvature
Annexin A5	1.33 ± 0.009	8-13	iTRAQ	+	Yes	Membrane Curvature

FIGURE 1. **Quantitative proteomics reveals the repertoire of proteins exhibiting increased levels in αβγ-synuclein KO synapses.** *A*, DIGE gel of the synaptic vesicle (*LP2*) fraction. The image is a scan of the αβγ-synuclein KO sample, and the spots corresponding to the location of α- and β-synuclein are highlighted in *red*. A total of 6 DIGE experiments were performed and quantitatively compared all synaptic fractions. On average, we analyzed ~50 proteins/DIGE experiment. *B*, volcano plot of iTRAQ experiment on synaptic cytosol fraction (*LS2*). The frequency distribution of peptides showing differences between wild type and αβγ-synuclein KO samples, plotted as $\log_{10}$(WT/KO), are overlaid with the protein score for each protein. The largest changes were observed for α- and β-synuclein and are noted. Note that most protein levels are unchanged and thus center around $\log_{10}$(WT/KO) = 0. A total of 6 iTRAQ experiments were conducted, and we analyzed ~500 proteins/iTRAQ experiment. *C*, table showing proteins that were increased in αβγ-synuclein KO synapses. Only proteins that were increased beyond cut-offs whose change was replicated in at least two biological and technical replicates are included. The average fold increase ± S.E., the number of peptides used to identify a given protein, the method by which the protein change was determined, if the change was validated, the lipid binding properties, and known functions of the proteins are listed. We validated the increase in protein levels for endophilin A1, endophilin B2, annexin A5, and synapsin IIb by quantitative immunoblotting, which is indicated by a + sign (See Fig. 2 and Ref. 12).

Electron Microscopy—Liposome tubulation was imaged with electron microscopy following the protocol from Ref. 34.

RESULTS

Endophilin Protein Expression Undergoes Compensatory Up-regulation Upon Loss of Synucleins—Quantitative proteomics affords an unbiased and sensitive way to monitor global protein changes. In the case of synucleins, it allows us to identify other proteins affected by deletion of synucleins, thus indicating possible functions. To identify such protein alterations, we performed DIGE (two-dimensional fluorescence difference gel electrophoresis) and iTRAQ (Isobaric Tag for Relative and Absolute Quantitation) on wild type and αβγ-synuclein KO synaptic fractions (Fig. 1). DIGE and iTRAQ use differential tags, fluorescent and isobaric respectively, to monitor protein changes and are used in a complementary manner (37). In both methods, as expected, the largest changes were observed for α- and β-synuclein (Fig. 1, *A* and *B*). We set stringent criteria to denote genuine protein changes, including strict cut-offs and replication in both biological ($n = 3$) and technical ($n = 2–4$) replicates. Interestingly, there were very few other protein changes in αβγ-synuclein KO samples. The only proteins that were consistently increased were the endocytic N-BAR protein endophilin A1 and its family member endophilin B2, the peripherally associated synaptic vesicle protein synapsin IIb, and the phosphatidylserine-binding protein annexin A5 (Fig. 1*C*). The increase in the levels of these four proteins was modest, in the range of 1.26–1.74-fold in αβγ-synuclein KO synaptic fractions. We validated the mass spectrometry results for all four proteins by quanititative immunoblotting (*validated column*, Fig. 1*C*). The observed increase for synapsin IIb is consistent with our previously published results (12). Notably, all of the proteins identified to be up-regulated in αβγ-synuclein KO synapses have several common biochemical features including negatively charged phospholipid binding and membrane curvature sensing/generation (34, 38–41), suggesting that these are shared properties and functions of synucleins.

As two members of the endophilin family were up-regulated in the αβγ-synuclein KO proteomic screen (Fig. 1), we investi-

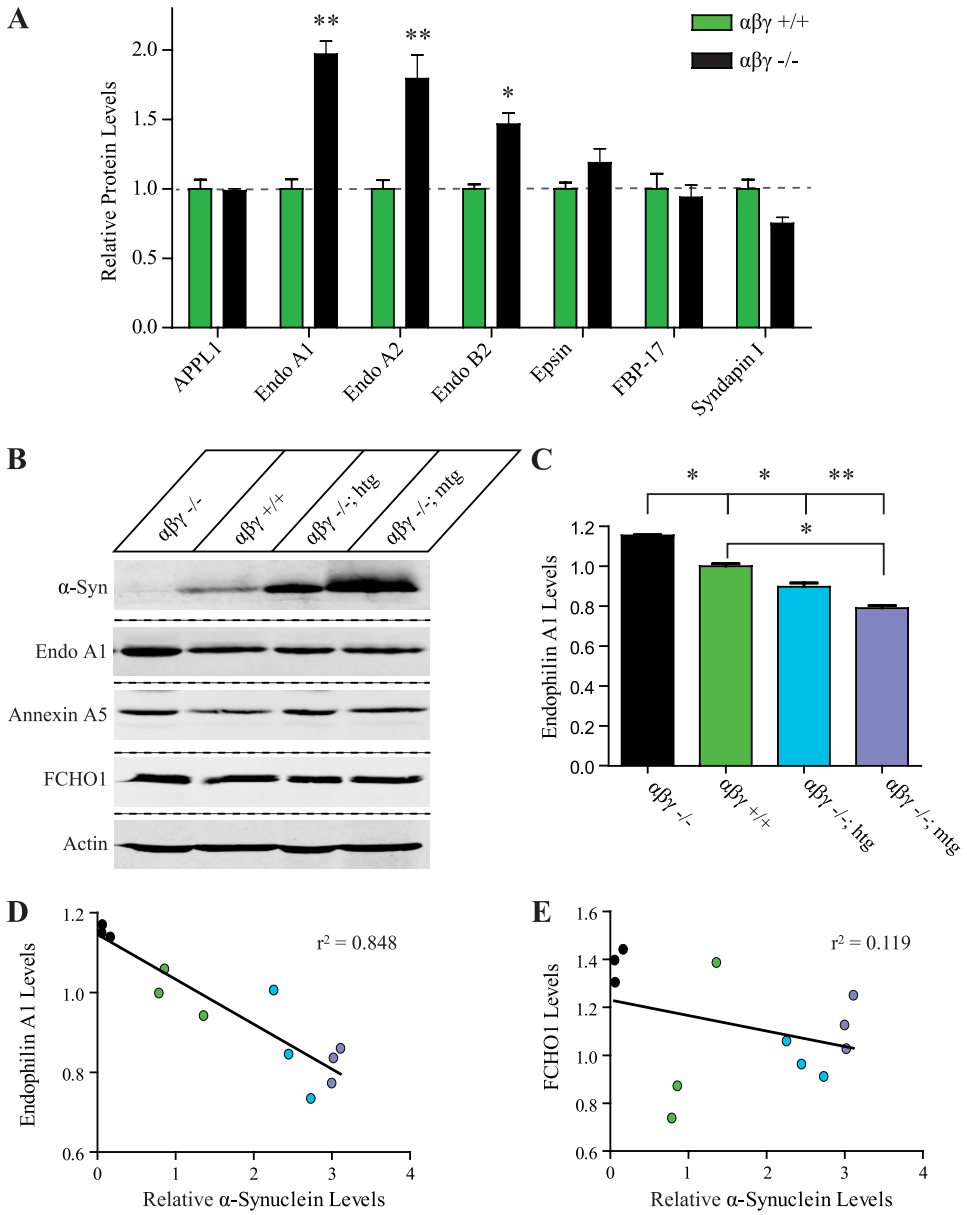

FIGURE 2. **Proteomic analysis reveals that synucleins and endophilin A1 levels are inversely related.** *A*, validation of endophilin levels by quantitative immunoblotting. Wild type (*green bar*) and $\alpha\beta\gamma$-synuclein KO (*black bar*; $n = 4$/genotype) brain homogenates (20 μg protein) were separated on SDS-PAGE gels and immunoblotted for the denoted proteins. The levels of individual proteins were determined by quantitative Western blotting with IRDye conjugated secondary antibodies on a LI-COR infrared imaging system, using actin and tubulin as internal loading controls. Abbreviations: *Endo*, endophilin; *, $p < 0.05$, **, $p < 0.01$. *B*, representative Western blot of synaptic protein expression of endophilin A1, annexin A5, and FCHO1 in age-matched $\alpha\beta\gamma$-synuclein KO ($\alpha\beta\gamma -/-$), wild type ($\alpha\beta\gamma +/+$), transgenic human ($\alpha\beta\gamma -/-$; htg) and mouse ($\alpha\beta\gamma -/-$; mtg) α-synuclein overexpression mouse models ($n = 3$/genotype). Actin is used as a loading control. *C*, quantification of endophilin A1 levels in $\alpha\beta\gamma$-synuclein KO, wild type, and α-synuclein overexpression mouse models. *, $p < 0.05$, **, $p < 0.01$. *D*, comparison of synaptic protein expression shows an inverse relationship between α-synuclein and endophilin A1 levels. $r^2 = 0.848$. See supplemental Fig. S2 for a similar analysis using total brain homogenates. *E*, levels of FCHO1 are unchanged as a function of α-synuclein levels. $r^2 = 0.119$.

gated the relationship between endophilins and synucleins. First, the increase in endophilin A1 and B2 levels was confirmed by quantitative immunoblotting of wild type and $\alpha\beta\gamma$-synuclein KO in total brain homogenates (1.97 ± 0.094- and 1.46 ± 0.079-fold, respectively; Fig. 2*A*). The magnitude of the increase was greater in the brain than in synaptic fractions as measured by mass spectrometry. Interestingly, we observed that the protein level of the closely related family member endophilin A2 was similarly increased (1.79 ± 0.169; Fig. 2*A*). We also saw that other membrane curvature inducing proteins such as the N-BAR protein APPL1, the F-BAR proteins synaptojpin I and FBP-17, and the amphipathic helix-containing protein epsin were unchanged (Fig. 2*A*; Refs. 42, 43), corroborating the DIGE and iTRAQ data. These data suggest that the endophilin family of proteins undergo compensatory up-regulation upon loss of synucleins.

To test *in vivo* to what extent the increases in endophilin A1 were synuclein-dependent, we examined endophilin A1 levels in synaptosomes of wild type, $\alpha\beta\gamma$-synuclein KO and two lines of rescued $\alpha\beta\gamma$-synuclein KO mice. The rescued mice are $\alpha\beta\gamma$-synuclein triple KO mice that express either a human or mouse wild type α-synuclein transgene pan-neuronally (28). Expres-

sion of these transgenes restores deficits caused by deletion of synucleins such as decreased synapse size and altered neurotransmission (12). Endophilin A1 levels were increased in $\alpha\beta\gamma$-synuclein KO synaptosomes (1.15 ± 0.005) as expected, by a magnitude similar to that seen in the iTRAQ experiments (Fig. 1*C*). Interestingly, increasing synuclein levels by transgenic expression reduced endophilin A1 levels even below wild type levels (Fig. 2, *B* and *C*). This was seen in both lines of rescued mice as compared with $\alpha\beta\gamma$-synuclein KOs (Fig. 2, *B* and *C*). To investigate this further, we plotted endophilin A1 and F-BAR protein FCHO1 levels against increasing α-synuclein levels seen in the $\alpha\beta\gamma$-synuclein KO, wild type, human and mouse α-synuclein transgene rescued synuclein KOs. The resulting graph reveals an inverse correlation between α-synuclein and endophilin A1 ($r^2 = 0.848$; Fig. 2*D*) but not FCHO1 levels ($r^2 = 0.119$; Fig. 2*E*). We also observed a comparable relationship between α-synuclein and endophilin in total brain homogenates from these mice (supplemental Fig. S2). We next investigated the relationship between endophilin B2 and α-synuclein levels and observed a similar inverse trend (data not shown). However, these data were not conclusive due to the poor quality of available endophilin B2 antibodies. Interestingly, annexin A5, whose levels are increased in $\alpha\beta\gamma$-synuclein null mice, does not exhibit an inverse relationship to α-synuclein levels (Fig. 2*B*, correlation with α-synuclein levels has $r^2 = 0.234$). Thus it appears that there is specificity to the endophilin-synuclein relationship and that neurons regulate the levels of endophilin A1 based on synuclein levels. We determined that the changes in endophilin A1, A2, and B2 levels occurs post-transcriptionally (SSC)[4]. Taken together, these results suggest that synucleins and endophilin A1 proteins are functionally related, and neurons maintain a constant level of these proteins collectively.

Synucleins Generate Membrane Curvature in Vitro—Endophilin A1 senses and generates membrane curvature through insertion of its N-terminal helix (H0) as well as scaffolding the membrane via its BAR domain (38, 44). Based on our finding that the levels of synucleins are inversely correlated with endophilin levels *in vivo*, we tested if synucleins can generate membrane curvature under physiological conditions. We utilized a membrane tubulation assay that has been extensively used to monitor the membrane-deforming properties of N-BAR domain proteins (36). In this assay, fluorescently labeled liposomes are mixed with purified proteins (supplemental Fig. S1*B*), and membrane curvature generation is visualized as formation of lipid tubules.

Membrane curvature generation is highly dependent on membrane composition, membrane rigidity, *i.e.* percentage of cholesterol, and protein concentration. We tested if human synucleins can evaginate membranes of different membrane compositions. Initially, we conducted this assay with liposomes composed of a synthetic lipid mixture (DOPE: DOPS: cholesterol 50:40:10; 1 mg/ml) that has a high propensity to deform. As seen in representative images in Fig. 3*A*, human α-, β-, and γ-synuclein at a concentration of 1.4 μM (molar lipid/protein ratio of ~1000:1) each can readily generate membrane tubules similar to endophilin A1, while BSA is unable to do so. Importantly, we next tested if membranes akin to those at the synaptic terminal can also be deformed by synucleins. Liposomes derived from brain polar lipid extracts (BPL; 1 mg/ml) were fluorescently labeled and mixed with recombinantly purified synucleins and endophilin A1 (molar lipid/protein ratio of ~1000:1). Again, all human synucleins robustly generated membrane curvature (Fig. 3*B*), suggesting that synuclein can act upon synaptic membranes. We also demonstrated that mouse synucleins can generate membrane curvature (supplemental Fig. S3), clearly indicating that this is a property shared by synucleins across species.

We quantified membrane tubulation from randomly selected images and observed that α-, β-, and γ-synuclein have a comparable membrane tubulation activity (Fig. 3*C*). As the N-terminal sequences of synucleins are the most conserved and involved in membrane binding, tubulation is therefore likely to be mediated by this sequence. Synuclein tubulation activity was ~2.5-fold less efficient than that of endophilin A1 (Fig. 3*C*). This is probably attributable to the fact that synucleins can generate membrane curvature only by wedging their N-terminal amphipathic helix into the membrane, while endophilin A1, in addition to using the wedge mechanism, also scaffolds membranes via its BAR domain (38, 44). We also demonstrated that synucleins directly participate in membrane tubulation as they are present on membrane tubules as shown using Alexa 488-conjugated α-synuclein (Fig. 3*D*). These data strongly suggest that synucleins can generate membrane curvature through insertion of their conserved, amphipathic N-terminal helices.

The fluorescence images of membrane tubules are diffraction limited; in order to obtain a more detailed image of synuclein-generated tubules, we visualized these structures by negative staining and electron microscopy. In the absence of synucleins, the liposomes are spherical (Fig. 4*A*). Incubation of liposomes with α-, β-, or γ-synuclein for 10 min at 37 °C results in evagination of liposomes into narrow tubules (Fig. 4, *B–D*), consistent with our confocal imaging results. Interestingly, synuclein-generated tubules showed much greater heterogeneity compared with the uniform, homogeneous tubules characteristic of endophilin A1 (Fig. 4, Ref. 34).

Membrane curvature generation is influenced not only by membrane composition but also protein concentration. The ability of a protein to sense *versus* generate curvature is strictly dependent on the concentration of the membrane bending protein, with higher concentrations needed for membrane curvature generation (45, 46). Hence, we wanted to determine the concentration dependence of synuclein tubulation activity and verify if it is within the range of synuclein concentration found at the synapse. We utilized the fluorescent BPL liposome assay to determine the α-synuclein concentration dependence of membrane tubulation. The extent of membrane tubulation increases linearly with α-synuclein concentration in the low micromolar range but saturates around 15 μM (Fig. 5*A*). To evaluate if this result was physiologically relevant, we next ascertained the synaptic concentrations of synucleins.

We used quantitative immunoblotting with purified protein standards and α-synuclein-specific antibodies to determine the

[4] Yongquan Zhang and S.S.C., personal communication.

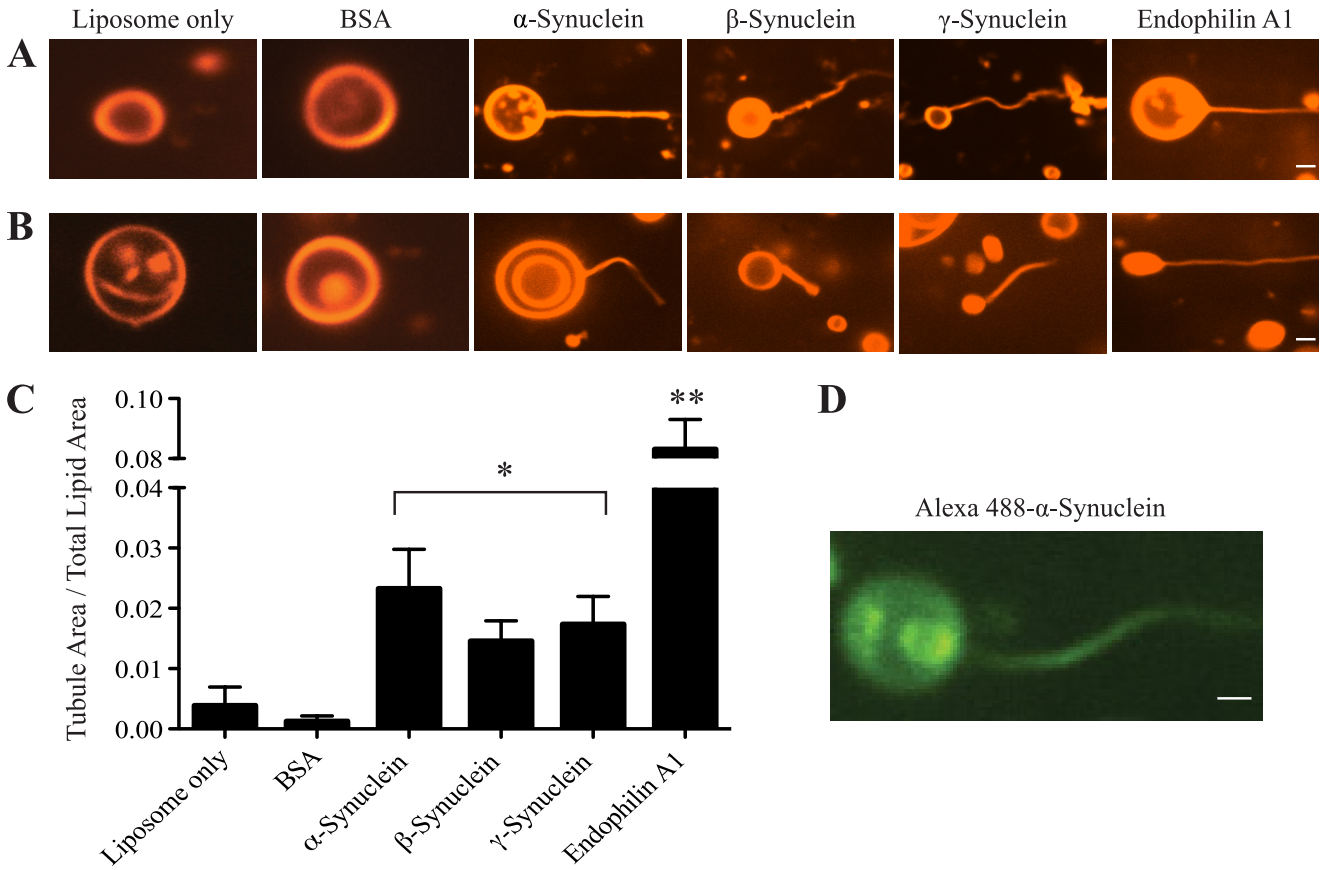

FIGURE 3. **All synucleins generate membrane curvature *in vitro*.** Images of liposomes only and liposomes mixed with BSA, α-, β-, γ-synuclein and endophilin A1. Tubules were generated by α-, β-, γ-synucleins and endophilin A1 (1.4 μM) from rhodamine-labeled liposomes composed of either: *A*, 50% DOPE/40% DOPS/10% cholesterol (1 mg/ml) or *B*, brain polar lipid (BPL; 1 mg/ml). Scale bar = 1 μm and applies to all images in a given row. *C*, quantification of tubulation activity, as measured by the ratio of tubule area to total lipid area for BSA, synucleins, and endophilin A1 using BPL-derived liposomes. BSA and endophilin A1 were used as negative and positive controls, respectively. Liposome-only and synuclein ratios are calculated from 900 images each, BSA and endophilin A1 from 540 images each; *, $p < 0.05$; **, $p < 0.01$ for comparisons to the liposomes only condition. *D*, Alexa-fluor 488-labeled α-synuclein localizes on the membrane tubules generated. Scale bar = 1 μm.

concentration of synuclein at the synapse (Fig. 5, *B* and *C*). The concentration of α-synuclein in brain homogenate was high at 0.03% of total brain protein, largely consistent with published literature (47). We then extrapolated the synaptic α-synuclein protein concentration by Western blotting purified synaptosomes for α-synuclein and approximating the volume of synapses at 0.12× of the total brain volume (assuming a uniform distribution of proteins in the brain). Based on this assumption, the concentration of α-synuclein is 4.5 ± 1.1 μM, more than sufficient to tubulate membranes robustly. In an independent approach, we estimated α-synuclein concentration by a comparison with other synaptic proteins whose concentrations have been well-established. We chose synaptobrevin 2 as it is the most abundant synaptic vesicle protein, with 70 synaptobrevin 2 molecules per synaptic vesicle (48). Assuming an average of 500 vesicles/synapse (49) and the volume of an average synapse to be 0.176 μm^3 based on synaptic morphometric measurements (12, 50), the volume of synapses was calculated to be 0.07 of total brain volume (supplemental Fig. S4). Using this ratio, the calculated concentration of α-synuclein is 2.6 ± 0.8 μM, again well within the range in which α-synuclein tubulates membranes *in vitro* (Fig. 5*A*). α-Synuclein concentrations at the synapse can therefore be expected to be in the range of 2–5 μM. Expression of α-synuclein closely overlaps with β-synuclein (51), hence the combined synuclein concentration is likely to be higher. Furthermore, synucleins are not uniformly distributed in the synapse but concentrated on vesicles and membranes (24), which means that the effective local concentration at the membrane is expected to be significantly higher than the above estimate. Together, these data corroborate the hypothesis that synucleins can generate membrane tubulation at concentrations found at the synapse.

Characterization of the Native α-Synuclein Tetramer—Recently, a novel physiological α-synuclein species, a natively folded tetramer, was identified (16). To better understand this newly identified α-synuclein species, we purified the α-synuclein tetramer from freshly drawn human blood following the protocol of Ref. 16 (supplemental Fig. S5; Fig. 6*A*). The α-synuclein tetramer could be purified as an intact species and separated from monomer by sequential chromatography. Employing crosslinking and circular dichroism, we confirmed that the α-synuclein species purified from blood is a folded tetramer (Fig. 6, *A* and *B*), as described (16). Published NMR analysis of the natively folded α-synuclein tetramer revealed that the N-terminal amphipathic helices are engaged in neighboring subunit interactions (17), yet tetrameric α-synuclein binds acidic lipid membranes with greater affinity than monomeric α-synuclein (16). Due to these apparently contradictory prop-

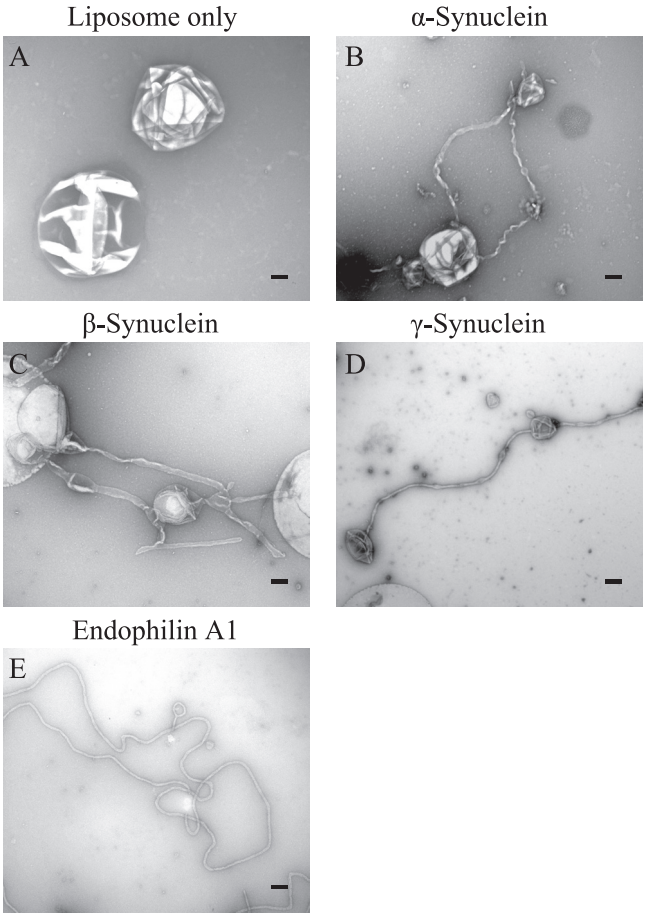

FIGURE 4. **Electron microscopic analysis of synuclein-generated tubules.** Representative electron micrographs of membrane tubules generated by: *A*, liposomes; *B*, α-synuclein; *C*, β-synuclein; *D*, γ-synuclein; and *E*, endophilin A1 using the 50%DOPE/40%DOPS/10% cholesterol liposomes. Scale bar = 100 nm. Similar results were obtained in three independent experiments.

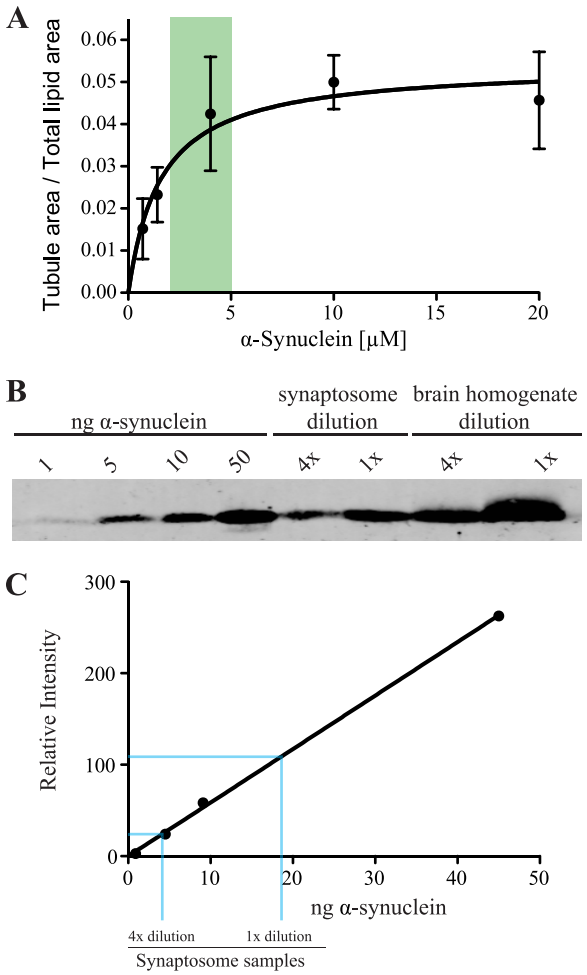

FIGURE 5. **Concentration dependence of α-synuclein generated membrane tubulation.** *A*, dose dependence of α-synuclein-mediated membrane tubulation. The tubulation activity of α-synuclein at the denoted protein concentrations was quantified as described in Fig. 3. Membrane tubulation shows a linear relationship to α-synuclein concentration until ~7 μM and saturates around 15 μM. Ratios are calculated from at least 540 images for each concentration. The *green-shaded area* represents the concentration of α-synuclein at the synapse. *B*, representative Western blot of α-synuclein standards, along with undiluted (1×) and diluted (4×) synaptosomes and total brain homogenate, blotted with a mouse α-synuclein specific antibody. These blots were used to compare and estimate the concentration of α-synuclein at synapses and in brain homogenate. *C*, standard curve for synaptosome samples generated from quantifying blots shown in *B*. ($r^2 = 0.991$). *Blue lines* indicate the amount of α-synuclein in undiluted (1×) and diluted (4×) synaptosomes. See supplemental Fig. S4 for a similar analysis using synaptobrevin 2 standards.

erties, it is not clear if the native tetramer can support membrane tubulation. By use of the fluorescence tubulation assay, we examined whether human tetrameric α-synuclein can generate membrane curvature. As seen in Fig. 6*C*, tetrameric α-synuclein is clearly deficient in this activity. A side-by-side comparison of tetrameric and monomeric α-synuclein at the same molar concentration using the same liposome samples shows that the tetrameric α-synuclein is unable to tubulate membranes, and has a tubule area/total lipid area ratio similar to that of liposomes alone (Fig. 3*C*). This result clearly shows that tetrameric and monomeric α-synuclein have distinct biochemical properties in regard to their interactions with membranes.

The A30P PD Mutant Is Defective in Membrane Tubulation—The human *PARK4* mutations, duplications and triplications of the human α-synuclein gene, increase α-synuclein expression. The triplication patients exhibit 2-fold more α-synuclein protein (52, 53). Based on the concentration curve of α-synuclein membrane tubulation (Fig. 5*A*), the *PARK4* mutations would be expected to double or even saturate membrane tubulation activity. However, how the *PARK1* point mutations affect α-synuclein membrane tubulation is less clear. The three known mutations, A53T, A30P, and E46K, have different membrane binding properties, with the E46K mutant exhibiting slightly increased membrane binding, the A53T mutant binding comparable to wild type, and the A30P mutant showing diminished membrane binding (54–56). We tested the ability of these three PD mutants to bend membranes and tubulate BPL-derived liposomes. Our results show that the A53T and E46K mutants have membrane tubulation activity similar to wild type α-synuclein whereas the A30P has negligible membrane bending ability (Fig. 7). The observation that the E46K mutant did not exhibit increased membrane tubulation confirms that lipid affinity alone is not sufficient to drive membrane tubulation. In the A30P mutant, the lack of membrane tubulation activity may simply reflect diminished membrane binding. Previous data have shown that the affinity of the A30P mutant to membranes of a composition similar to those we used is ~50% of wild type α-synuclein (56). We therefore tested

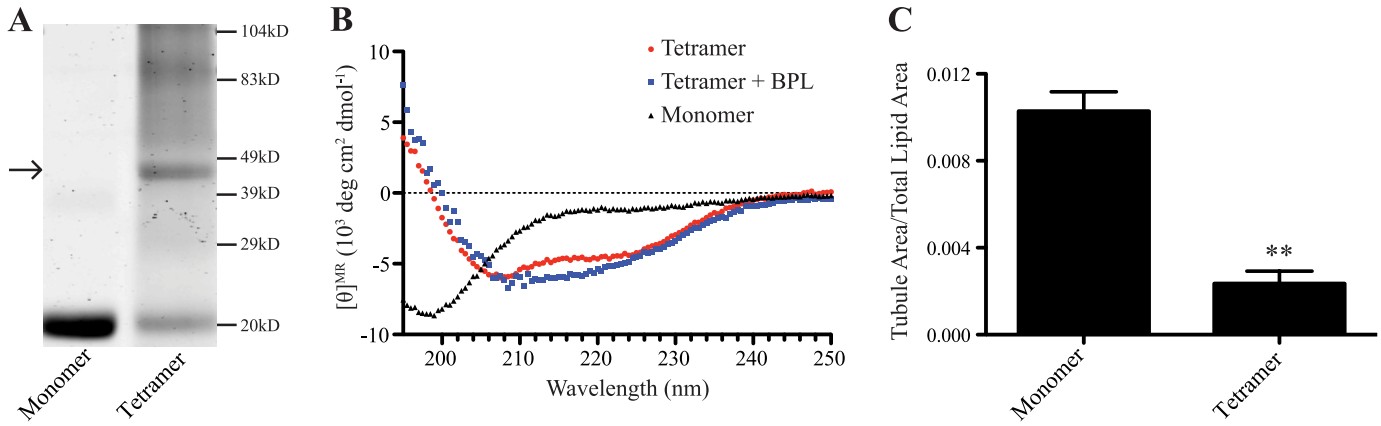

FIGURE 6. **Purification and characterization of the native α-synuclein tetramer.** *A*, crosslinking of recombinantly purified monomeric and blood purified tetrameric α-synuclein. The purified proteins were crosslinked with glutaraldehyde according to Ref. 16 and separated on SDS-PAGE. The gel shows a band of ~50 kDa corresponding to the tetramer (*arrow*), while the monomer remains at ~14kD. *B*, circular dichroism (*CD*) of tetrameric and monomeric α-synuclein. Spectra show the tetramer is folded in solution, and its folding is unchanged by the addition of BPL liposomes, while the recombinantly purified, monomeric α-synuclein is unfolded in solution. *C*, quantification of α-synuclein tetramer tubulation. Graph shows that the tetramer is unable to generate membrane curvature. Quantification of tubulation activity was done as described in Fig. 3 from 540 images for each condition. **, $p < 0.01$.

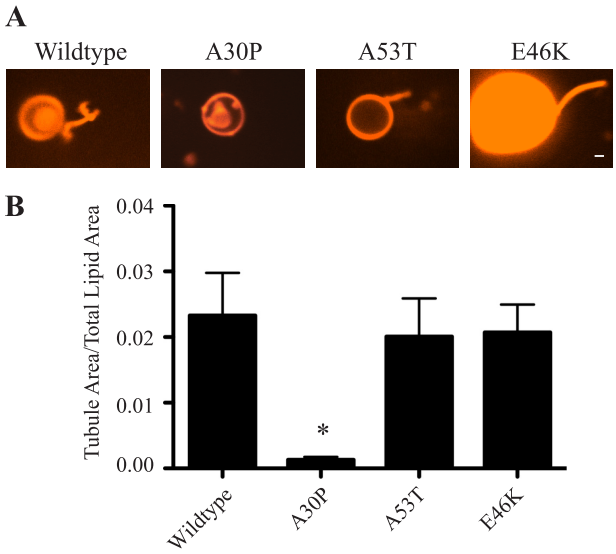

FIGURE 7. **PD mutants of α-synuclein have varied ability to generate membrane curvature.** *A*, representative images of membrane tubules generated by human wild type α-synuclein and the three PD mutants. *B*, quantification of membrane tubulation activity of the three human PD mutants as compared with human wild type α-synuclein. While A53T and E46K tubulation activity is similar to wild type, the A30P mutant has no membrane tubulation activity. Ratios were quantified from 540 images for each condition. *, $p < 0.05$.

if increasing the concentration of the mutant protein 2- 10-fold, while keeping the liposome concentration constant, could lead to membrane tubulation. Increasing A30P concentration shows a trend to increased membrane curvature generation, but the data are not significant (supplemental Fig. S6). Further, a comparison of wild type and A30P mutant protein at equivalent membrane bound levels shows that the A30P mutant is still deficient in membrane tubulation. These data suggest that the A30P mutation is a loss-of-function mutation in addition to being a toxic gain-of-function mutation, consistent with published mouse genetic data (28).

DISCUSSION

In this study, we sought to elucidate the molecular functions of synucleins. Using unbiased proteomics, we showed that four proteins that sense and generate membrane curvature, endophilin A1, endophilin B2, annexin A5, and synapsin IIb, are up-regulated upon the loss of synucleins, strongly suggesting that synucleins function similarly. We then determined by both fluorescence confocal microscopy and electron microscopy that all members of the synuclein family can readily generate membrane curvature when monomeric, extending previous results (25–27). Importantly, we quantitated this activity and demonstrated that α-, β-, and γ-synuclein can tubulate liposomes composed of naturally occurring brain lipids to comparable levels (Fig. 3*C*). Notably, synucleins bend membranes at concentrations likely to be present at synapses (Fig. 5). In marked contrast to monomeric synucleins, we show for the first time that a novel α-synuclein tetramer is unable to bend membranes (Fig. 6*C*).

Synucleins Sense and Generate Membrane Curvature Similar to Other Amphipathic Helical Proteins—Our data suggest that synucleins behave like other lipid-binding amphipathic helical proteins such as endophilin A1, epsin, and Arf1. It is well established for these proteins that they generate membrane curvature through asymmetric insertion of hydrophobic amino acids into the lipid membrane (34, 38, 43–45, 57). Previous structural studies have shown that when α-synuclein folds on membranes into an amphipathic helical conformation, it inserts into the outer leaflet of the membrane (19, 22, 27). Based on sequence and structural similarities it is predicted that β- and γ-synuclein behave alike (58). Thus synucleins share a key structural characteristic of this class of membrane curvature generating proteins. Another feature of this category of proteins is that they both sense and generate membrane curvature. Recent studies suggest that membrane curvature sensing and generation occurs through the same physicochemical interactions with lipid membranes, and whether a given protein does one or both of these functions depends mainly on protein concentration and bound density (46). Our findings that all synucleins generate membrane curvature along with previous results that synucleins sense curvature (15, 23, 25–27) indicate that synucleins participate in both processes. We have estimated that the synaptic concentration of α-synuclein is in the range of 2–5 μM, more than adequate for membrane curvature

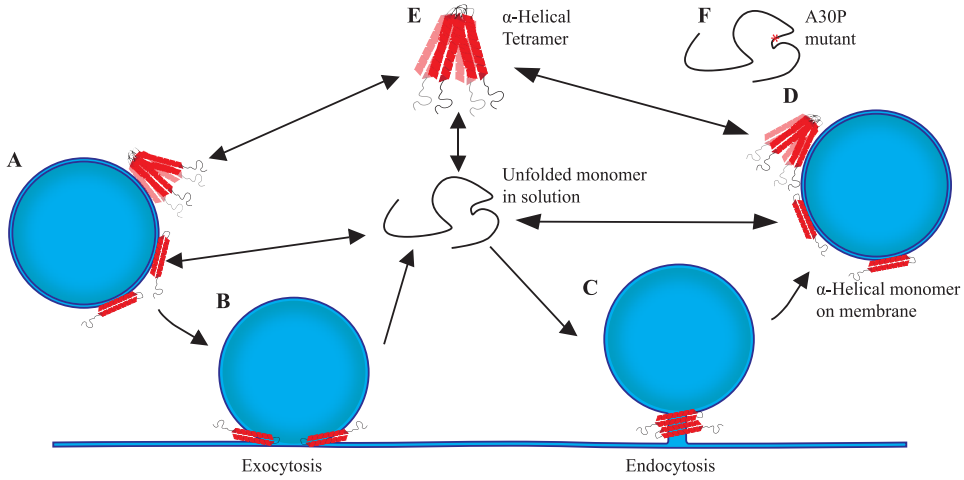

FIGURE 8. **Model of α-synuclein membrane curvature generation and its possible synaptic functions.** *A*, at rest, α-synuclein is on the synaptic vesicle in an α-helical conformation. *B*, upon stimulation, it generates curvature during exocytosis, after which it comes off the flattened membrane and becomes unfolded. *C*, at the start of endocytosis, α-synuclein binds to the incipiently curved membrane to generate further curvature at the endocytic stalk. *D*, after one round of neurotransmitter release, it is bound to the synaptic vesicle again. *E*, unused α-synuclein is stored as a folded tetramer. *F*, the A30P PD mutant of α-synuclein does not participate in any of these membrane functions.

generation (Fig. 5). Taken together, our results put synucleins into the same class of amphipathic helix containing proteins that sense and generate membrane curvature.

Structural Requirements for Membrane Curvature Generation—The first 38 amino acids are required for α-synuclein to sense membrane curvature *in vivo* (59). Here we have provided three lines of evidence to suggest that the entire N-terminal region of synucleins is responsible for membrane curvature generation. (i) Membrane curvature generation is a shared biochemical property of all synucleins (Fig. 3). The N terminus of α-, β-, and γ- synuclein is the only region with high sequence homology among the family members (supplemental Fig. S1). The N termini of synucleins fold into an amphipathic helix upon lipid binding, while their C termini remain unstructured (18, 22, 58). (ii) The A30P mutation in α-synuclein that disrupts α-helix formation (20, 25) has minimal membrane tubulation activity (Fig. 7; supplemental Fig. S6). (iii) Tetramic α-synuclein, in which the N-terminal helices are engaged in protein-protein interactions (17), is also deficient in membrane curvature generation (Fig. 6). Recent continuous wave EPR measurements confirm that α-synuclein adopts an uninterrupted N-terminal α-helical conformation on synthetic lipid tubules (58).

Is the α-Synuclein Tetramer a Physiological Species?—Monomeric α-synuclein, in addition to exhibiting conformational plasticity (60), readily forms higher order β-rich oligomers and eventually the large-scale β-sheeted structures observed in Lewy bodies. Until the identification of the native α-synuclein tetramer, the higher order oligomers were thought to be pathogenic species. Since its discovery there has been much discussion whether the α-synuclein tetramer is a physiologically-relevant species. We were therefore keen to characterize the membrane tubulation properties of this novel α-synuclein tetramer. We successfully purified the tetramer from human blood (Fig. 6, *A* and *B*; supplemental Fig. S5). The tetramer was natively folded, in an α-helical conformation, and could bind lipids. However, in the fluorescent tubulation assay, tetrameric α-synuclein clearly could not tubulate membranes (Fig. 6*C*). This would be consistent with the idea that the native tetramer is acting as an inert reservoir of monomeric α-synuclein (Fig. 8*E*). This concept is supported by the observation that the yield of the tetramer is low, suggesting that the tetramer can readily dissociate to monomers. Furthermore, while we can purify the tetramer from blood, it is not a predominant species in brain. *In situ* cross-linking experiments of synaptosomes clearly show the majority of α-synuclein in murine synapses is monomeric (supplemental Fig. S7). This has also been reported in a recent paper (61). Also, β- and γ-synuclein tetramers have not yet been identified, suggesting a lack of conservation. Based on our results, we propose that membrane-bound monomeric α-synuclein, and not tetrameric α-synuclein, is important for its synaptic functions.

Physiological Function of Synucleins and Their Role in Parkinson Disease—Synucleins are associated with synaptic vesicles and regulate their biological function (12). The synaptic vesicle cycle is an intricately orchestrated set of protein-protein and protein-lipid interactions regulated with exquisite spatial and temporal specificity. On the basis of six lines of evidence listed below, we postulate that synucleins function in synaptic vesicle exocytosis, endocytosis, or both (Fig. 8, *B* and *C*). (i) α-Synuclein has been shown to interact with SNAREs during synaptic vesicle exocytosis (11). Taken together with our results that synucleins bend synaptic membranes, it suggests that synucleins could coordinate membrane bending during exocytosis similar to other well-known exocytic proteins (62–64). (ii) Proteomic analysis of α-, β-, and γ- synuclein KO synapses revealed that levels of endophilin A1, a key endocytic protein, are significantly increased (Figs. 1 and 2), indicating that this N-BAR protein compensates for the loss of synucleins. (iii) The tubules generated by synucleins have been measured by cryoEM to have a diameter of 5–7 nm at saturation (27), but at physiological concentrations appear more varied in their width (Fig. 4, *B–D*). The width of these tubules is consistent with the neck of clathrin coated buds and suggests that synucleins could be active at endocytic sites along with endophilins (34). (iv) Synucleins bind the acidic phospholipid PIP_2, a key regulator of

endocytosis (65). (v) α-Synuclein is a component of clathrin-coated vesicles (66). (vi) Overexpression of α-synuclein rescues the synapse loss seen in knock-out mice for the co-chaperone CSPα (28) which participates in both exo- and endocytosis at the presynaptic terminal (31). Collectively, the above findings support the hypothesis that synucleins are participatants in the exo- and endocytic steps of the synaptic vesicle cycle. The possible roles of α-synuclein in curvature generation in exo- and endocytosis are depicted in a model in Fig. 8.

Our analysis of human PD mutants revealed that only the A30P mutant was unable to tubulate membranes (Fig. 7, supplemental Fig. S6). This is consistent with published literature that the A30P mutation disrupts α-helix formation and has weak membrane binding (28, 56, 67). In case of *PARK4* patients, increased expression of wild type human α-synuclein is likely to augment membrane bending, thus influencing synapse function. But in case of the *PARK1* mutations, A30P, A53T, and E46K, while all mutations cause PD, they had diametrically opposite effects on membrane tubulation. This suggests that membrane curvature generation is not related to the etiology of *PARK1* PD, but rather to the physiological function of synucleins at the presynaptic terminal.

Acknowledgments—We thank Min Wu, Michelle Pirruccello, Opeyemi Alabi, Ellen Vollmers, and Karina Vargas for help with the fluorescent membrane tubulation assay and visualization by electron microscopy; Terence Wu, Christopher Colangelo, and Kathy Stone for the DIGE and iTRAQ analysis; and Becket Greten-Harrison for quantitative immunoblotting. We thank Thomas Biederer, Pietro De Camilli, Art Horwich, H. Sharat Chandra, and other members of our laboratory for critically reading the manuscript.

REFERENCES

1. Spillantini, M. G., Schmidt, M. L., Lee, V. M., Trojanowski, J. Q., Jakes, R., and Goedert, M. (1997) α-Synuclein in Lewy bodies. *Nature* **388,** 839–840
2. Krüger, R., Kuhn, W., Müller, T., Woitalla, D., Graeber, M., Kösel, S., Przuntek, H., Epplen, J. T., Schöls, L., and Riess, O. (1998) A30P mutation in the gene encoding α-synuclein in Parkinson's disease. *Nat. Genet.* **18,** 106–108
3. Polymeropoulos, M. H., Lavedan, C., Leroy, E., Ide, S. E., Dehejia, A., Dutra, A., Pike, B., Root, H., Rubenstein, J., Boyer, R., Stenroos, E. S., Chandrasekharappa, S., Athanassiadou, A., Papapetropoulos, T., Johnson, W. G., Lazzarini, A. M., Duvoisin, R. C., Di Iorio, G., Golbe, L. I., and Nussbaum, R. L. (1997) Mutation in the α-synuclein gene identified in families with Parkinson's disease. *Science* **276,** 2045–2047
4. Zarranz, J. J., Alegre, J., Gómez-Esteban, J. C., Lezcano, E., Ros, R., Ampuero, I., Vidal, L., Hoenicka, J., Rodriguez, O., Atarés, B., Llorens, V., Gomez Tortosa, E., del Ser, T., Muñoz, D. G., and de Yebenes, J. G. (2004) The new mutation, E46K, of α-synuclein causes Parkinson and Lewy body dementia. *Ann. Neurol.* **55,** 164–173
5. Símon-Sánchez, J., Schulte, C., Bras, J. M., Sharma, M., Gibbs, J. R., Berg, D., Paisan-Ruiz, C., Lichtner, P., Scholz, S. W., Hernandez, D. G., Krüger, R., Federoff, M., Klein, C., Goate, A., Perlmutter, J., Bonin, M., Nalls, M. A., Illig, T., Gieger, C., Houlden, H., Steffens, M., Okun, M. S., Racette, B. A., Cookson, M. R., Foote, K. D., Fernandez, H. H., Traynor, B. J., Schreiber, S., Arepalli, S., Zonozi, R., Gwinn, K., van der Brug, M., Lopez, G., Chanock, S. J., Schatzkin, A., Park, Y., Hollenbeck, A., Gao, J., Huang, X., Wood, N. W., Lorenz, D., Deuschl, G., Chen, H., Riess, O., Hardy, J. A., Singleton, A. B., and Gasser, T. (2009) Genome-wide association study reveals genetic risk underlying Parkinson's disease. *Nat. Genet.* **41,** 1308–1312
6. Satake, W., Nakabayashi, Y., Mizuta, I., Hirota, Y., Ito, C., Kubo, M., Kawaguchi, T., Tsunoda, T., Watanabe, M., Takeda, A., Tomiyama, H., Nakashima, K., Hasegawa, K., Obata, F., Yoshikawa, T., Kawakami, H., Sakoda, S., Yamamoto, M., Hattori, N., Murata, M., Nakamura, Y., and Toda, T. (2009) Genome-wide association study identifies common variants at four loci as genetic risk factors for Parkinson's disease. *Nat. Genet.* **41,** 1303–1307
7. Murphy, D. D., Rueter, S. M., Trojanowski, J. Q., and Lee, V. M. (2000) Synucleins are developmentally expressed, and α-synuclein regulates the size of the presynaptic vesicular pool in primary hippocampal neurons. *J. Neurosci.* **20,** 3214–3220
8. Cabin, D. E., Shimazu, K., Murphy, D., Cole, N. B., Gottschalk, W., McIlwain, K. L., Orrison, B., Chen, A., Ellis, C. E., Paylor, R., Lu, B., and Nussbaum, R. L. (2002) Synaptic vesicle depletion correlates with attenuated synaptic responses to prolonged repetitive stimulation in mice lacking α-synuclein. *J. Neurosci.* **22,** 8797–8807
9. Anwar, S., Peters, O., Millership, S., Ninkina, N., Doig, N., Connor-Robson, N., Threlfell, S., Kooner, G., Deacon, R. M., Bannerman, D. M., Bolam, J. P., Chandra, S. S., Cragg, S. J., Wade-Martins, R., and Buchman, V. L. (2011) Functional alterations to the nigrostriatal system in mice lacking all three members of the synuclein family. *J. Neurosci.* **31,** 7264–7274
10. Ben Gedalya, T., Loeb, V., Israeli, E., Altschuler, Y., Selkoe, D. J., and Sharon, R. (2009) α-Synuclein and polyunsaturated fatty acids promote clathrin-mediated endocytosis and synaptic vesicle recycling. *Traffic* **10,** 218–234
11. Burré, J., Sharma, M., Tsetsenis, T., Buchman, V., Etherton, M. R., and Südhof, T. C. (2010) α-Synuclein promotes SNARE-complex assembly *in vivo* and *in vitro*. *Science* **329,** 1663–1667
12. Greten-Harrison, B., Polydoro, M., Morimoto-Tomita, M., Diao, L., Williams, A. M., Nie, E. H, Makani, S., Tian, N., Castillo, P. E., Buchman, V. L., Südhof, T. C., and Chandra, S. S. (2010) αβγ-Synuclein triple knockout mice reveal age-dependent neuronal dysfunction. *Proc. Natl. Acad. Sci. U.S.A.* **107,** 19573–19578
13. Nemani, V. M., Lu, W., Berge, V., Nakamura, K., Onoa, B., Lee, M. K., Chaudhry, F. A., Nicoll, R. A., and Edwards, R. H. (2010) Increased expression of alpha-synuclein reduces neurotransmitter release by inhibiting synaptic vesicle reclustering after endocytosis. *Neuron* **65,** 66–79
14. Gaugler, M. N., Genc, O., Bobela, W., Mohanna, S., Ardah, M. T., El-Agnaf, O. M., Cantoni, M., Bensadoun, J. C., Schneggenburger, R., Knott, G. W., Aebischer, P., and Schneider, B. L. (2012) Nigrostriatal overabundance of α-synuclein leads to decreased vesicle density and deficits in dopamine release that correlate with reduced motor activity. *Acta Neuropathol.* **123,** 653–669
15. Davidson, W. S., Jonas, A., Clayton, D. F., and George, J. M. (1998) Stabilization of α-Synuclein in secondary structure upon binding to synthetic membranes. *J. Biol. Chem.* **273,** 9443–9449
16. Bartels, T., Choi, J. G., and Selkoe, D. J. (2011) α-Synuclein occurs physiologically as a helically folded tetramer that resists aggregation. *Nature* **477,** 107–110
17. Wang, W., Perovic, I., Chittuluru, J., Kaganovich, A., Nguyen, L. T., Liao, J., Auclair, J. R., Johnson, D., Landeru, A., Simorellis, A. K., Ju, S., Cookson, M. R., Asturias, F.J., Agar, J. N., Webb, B. N, Kang, C., Ringe, D., Petsko, G. A., Pochapsky, T. C., Hoang, Q. Q. (2011) A soluble α-synuclein construct forms a dynamic tetramer. *Proc. Natl. Acad. Sci. U.S.A.* **108,** 17797–17802
18. Chandra, S., Chen, X., Rizo, J., Jahn, R., and Südhof, T. C. (2003) A broken α-helix in folded α-synuclein. *J. Biol. Chem.* **278,** 15313–15318
19. Jao, C. C., Der-Sarkissian, A., Chen, J., and Langen, R. (2004) Structure of membrane-bound α-synuclein studied by site-directed spin labeling. *Proc. Natl. Acad. Sci. U.S.A.* **101,** 8331–8336
20. Ulmer, T. S., Bax, A., Cole, N. B., and Nussbaum, R. L. (2005) Structure and dynamics of micelle-bound human α-synuclein. *J. Biol. Chem.* **280,** 9595–9603
21. Ferreon, A. C., Gambin, Y., Lemke, E. A., and Deniz, A. A. (2009) Interplay of α-synuclein binding and conformational switching probed by single-molecule fluorescence. *Proc. Natl. Acad. Sci. U.S.A.* **106,** 5645–5650
22. Jao, C. C., Hegde, B. G., Chen, J., Haworth, I. S., and Langen, R. (2008) Structure of membrane-bound α-synuclein from site-directed spin labeling and computational refinement. *Proc. Natl. Acad. Sci. U.S.A.* **105,**

19666–19671
23. Middleton, E. R., and Rhoades, E. (2010) Effects of curvature and composition on α-synuclein binding to lipid vesicles. *Biophys. J.* **99,** 2279–2288
24. Clayton, D. F., and George, J. M. (1999) Synucleins in synaptic plasticity and neurodegenerative disorders. *J. Neurosci. Res.* **58,** 120–129
25. Varkey, J., Isas, J. M., Mizuno, N., Jensen, M. B., Bhatia, V. K., Jao, C. C., Petrlova, J., Voss, J. C., Stamou, D. G., Steven, A. C., and Langen, R. (2010) Membrane curvature induction and tubulation are common features of synucleins and apolipoproteins. *J. Biol. Chem.* **285,** 32486–32493
26. Pandey A. P., Haque, F., Rochet J. C., Hovis J. S. (2011) α-Synuclein-induced tubule formation in lipid bilayers. *J. Phys. Chem. B* **115,** 5886–5893
27. Mizuno, N., Varkey, J., Kegulian, N. C., Hegde, B. G., Cheng, N., Langen, R., Steven, A. C. (2012) Remodeling of lipid vesicles into cylindrical micelles by α-synuclein in an extended α-helical conformation. *J. Biol. Chem.* **287,** 29301–29311
28. Chandra, S., Gallardo, G., Fernández-Chacón, R., Schlüter, O. M., and Südhof, T. C. (2005) α-Synuclein cooperates with CSPα in preventing neurodegeneration. *Cell* **123,** 383–396
29. Huttner, W. B., Schiebler, W., Greengard, P., and De Camilli, P. (1983) Synapsin I (protein I), a nerve terminal-specific phosphoprotein. III. Its association with synaptic vesicles studied in a highly purified synaptic vesicle preparation. *J. Cell Biol.* **96,** 1374–1388
30. Wu, T. L. (2006) Two dimensional difference gel electrophoresis. *New Emerging Proteomics Techniques* **328,** 71–96
31. Zhang, Y. Q., Henderson, M. X., Colangelo, C. M., Ginsberg, S. D., Bruce, C., Wu, T., and Chandra, S. S. (2012) Identification of CSPα clients reveals a role in dynamin 1 regulation. *Neuron* **74,** 136–150
32. Dávalos, A., Fernández-Hernando, C., Sowa, G., Derakhshan, B., Lin, M. I., Lee, J. Y., Zhao, H., Luo, R., Colangelo, C., and Sessa, W. C. (2010) Quantitative proteomics of caveolin-1-regulated proteins: characterization of polymerase I and transcript release factor/CAVIN-1 in endothelial cells. *Mol. Cell Proteomics* **9,** 2109–2124
33. Shilov, I. V., Seymour, S. L., Patel, A. A., Loboda, A., Tang, W. H., Keating, S. P., Hunter, C. L., Nuwaysir, L. M., and Schaeffer, D. A. (2007) The Paragon Algorithm, a next generation search engine that uses sequence temperature values and feature probabilities to identify peptides from tandem mass spectra. *Mol. Cell Proteomics* **6,** 1638–1655
34. Farsad, K., Ringstad, N., Takei, K., Floyd, S. R., Rose, K., and De Camilli, P. (2001) Generation of high curvature membranes mediated by direct endophilin bilayer interactions. *J. Cell Biol.* **155,** 193–200
35. Takei, K., Slepnev, V. I., Haucke, V., and De Camilli, P. (1999) Functional partnership between amphiphysin and dynamin in clathrin-mediated endocytosis. *Nat. Cell Biol.* **1,** 33–39
36. Itoh, T., Erdmann, K. S., Roux, A., Habermann, B., Werner, H., and De Camilli, P. (2005) Dynamin and the actin cytoskeleton cooperatively regulate plasma membrane invagination by BAR and F-BAR proteins. *Dev. Cell* **9,** 791–804
37. Tannu, N. S., and Hemby, S. E. (2006) Methods for proteomics in neuroscience. *Prog Brain Res.* **158,** 41–82
38. Gallop, J. L., Jao, C. C., Kent, H. M., Butler, P. J., Evans, P. R., Langen, R., and McMahon, H. T. (2006) Mechanism of endophilin N-BAR domain-mediated membrane curvature. *EMBO J.* **25,** 2898–2910
39. Haucke, V., Neher, E., and Sigrist, S. J. (2011) Protein scaffolds in the coupling of synaptic exocytosis and endocytosis. *Nat. Rev. Neurosci.* **12,** 127–138
40. Hosaka, M., Hammer, R. E., and Südhof, T. C. (1999) A phospho-switch controls the dynamic association of synapsins with synaptic vesicles. *Neuron* **24,** 377–387
41. Oling, F., Santos, J. S., Govorukhina, N., Mazères-Dubut, C., Bergsma-Schutter, W., Oostergetel, G., Keegstra, W., Lambert, O., Lewit-Bentley, A., and Brisson, A. (2000) Structure of membrane-bound annexin A5 trimers: a hybrid cryo-EM - X-ray crystallography study. *J. Mol. Biol.* **304,** 561–573
42. Henne, W. M., Kent, H. M., Ford, M. G., Hegde, B. G., Daumke, O., Butler, P. J., Mittal, R., Langen, R., Evans, P. R., and McMahon, H. T. (2007) Structure and analysis of FCHo2 F-BAR domain: a dimerizing and membrane recruitment module that effects membrane curvature. *Structure* **15,** 839–852
43. Ford, M. G., Mills, I. G., Peter, B. J., Vallis, Y., Praefcke, G. J., Evans, P. R., and McMahon, H. T. (2002) Curvature of clathrin-coated pits driven by epsin. *Nature* **419,** 361–366
44. Mim, C., Cui, H., Gawronski-Salerno, J. A., Frost, A., Lyman, E., Voth, G. A., and Unger, V. M. (2012) Structural basis of membrane bending by the N-BAR protein endophilin. *Cell* **149,** 137–145
45. Drin, G., and Antonny, B. (2010) Amphipathic helices and membrane curvature. *FEBS Lett.* **584,** 1840–1847
46. Sorre, B., Callan-Jones, A., Manzi, J., Goud, B., Prost, J., Bassereau, P., and Roux, A. (2012) Nature of curvature coupling of amphiphysin with membranes depends on its bound density. *Proc. Natl. Acad. Sci. U.S.A.* **109,** 173–178
47. Nakajo, S., Tsukada, K., Kameyama, H., Furuyama, Y., and Nakaya, K. (1996) Distribution of phosphoneuroprotein 14 (PNP 14) in vertebrates: its levels as determined by enzyme immunoassay. *Brain Res.* **741,** 180–184
48. Takamori, S., Holt, M., Stenius, K., Lemke, E. A., Grønborg, M., Riedel, D., Urlaub, H., Schenck, S., Brügger, B., Ringler, P., Müller, S. A., Rammner, B., Gräter, F., Hub, J. S., De Groot, B. L., Mieskes, G., Moriyama, Y., Klingauf, J., Grubmüller, H., Heuser, J., Wieland, F., and Jahn, R. (2006) Molecular anatomy of a trafficking organelle. *Cell* **127,** 831–846
49. Jahn, R., and Südhof, T. C. (1993) Synaptic vesicle traffic: rush hour in the nerve terminal. *J. Neurochem.* **61,** 12–21
50. Fernandez-Busnadiego, R., Schrod, N., Kochovski, Z., Asano, S., Vanhecke, D., Baumeister, W., and Lucic, V. (2011) Insights into the molecular organization of the neuron by cryo-electron tomography. *J. Electron Microsc.* **60,** S137–S148
51. Abeliovich, A., Schmitz, Y., Fariñas, I., Choi-Lundberg, D., Ho, W. H., Castillo, P. E., Shinsky, N., Verdugo, J. M., Armanini, M., Ryan, A., Hynes, M., Phillips, H., Sulzer, D., and Rosenthal, A. (2000) Mice lacking α-synuclein display functional deficits in the nigrostriatal dopamine system. *Neuron* **25,** 239–252
52. Farrer, M., Kachergus, J., Forno, L., Lincoln, S., Wang, D. S., Hulihan, M., Maraganore, D., Gwinn-Hardy, K., Wszolek, Z., Dickson, D., Langston, J. W. (2004) Comparison of kindreds with parkinsonism and α-synuclein genomic multiplications. *Ann. Neurol.* **55,** 174–179
53. Miller, D. W., Hague, S. M., Clarimon, J., Baptista, M., Gwinn-Hardy, K., Cookson, M. R., Singleton, A. B. (2004) α-Synuclein in blood and brain from familial Parkinson disease with SNCA locus triplication. *Neurology* **62,** 1835–1838
54. Jensen, P. H., Nielsen, M. S., Jakes, R., Dotti, C. G., and Goedert, M. (1998) Binding of α-synuclein to brain vesicles is abolished by familial Parkinson's disease mutation. *J. Biol. Chem.* **273,** 26292–26294
55. Jo, E., Fuller, N., Rand, R. P., St George-Hyslop, P., and Fraser, P. E. (2002) Defective membrane interactions of familial Parkinson's disease mutant A30P α-synuclein. *J. Mol. Biol.* **315,** 799–807
56. Choi, W., Zibaee, S., Jakes, R., Serpell, L. C., Davletov, B., Crowther, R. A., Goedert, M. (2004) Mutation E46K increases phospholipid binding and assembly into filaments of human α-synuclein. *FEBS Lett.* **576,** 363–368
57. Yoon, Y., Tong, J., Lee, P. J., Albanese, A., Bhardwaj, N., Källberg, M., Digman, M. A., Lu, H., Gratton, E., Shin, Y. K., and Cho, W. (2010) Molecular basis of the potent membrane-remodeling activity of the epsin 1 N-terminal homology domain. *J. Biol. Chem.* **285,** 531–540
58. Sung, Y. H., and Eliezer, D. (2006) Secondary structure and dynamics of micelle bound β- and γ-synuclein. *Protein Sci.* **15,** 1162–1174
59. Pranke, I. M., Morello, V., Bigay, J., Gibson, K., Verbavatz, J. M., Antonny, B., and Jackson, C. L. (2011) α-Synuclein and ALPS motifs are membrane curvature sensors whose contrasting chemistry mediates selective vesicle binding. *J. Cell Biol.* **194,** 89–103
60. Drescher, M., Huber, M., and Subramaniam, V. (2012) Hunting the chameleon: structural conformations of the intrinsically disordered protein α-synuclein. *Chembiochem* **13,** 761–768
61. Fauvet, B., Mbefo, M. K., Fares, M. B., Desobry, C., Michael, S., Ardah, M. T., Tsika, E., Coune, P., Prudent, M., Lion, N., Eliezer, D., Moore, D. J., Schneider, B., Aebischer, P., El-Agnaf, O. M., Masliah, E., and Lashuel, H. A. (2012) α-Synuclein in central nervous system and from erythrocytes, mammalian cells, and *Escherichia coli* exists predominantly as disordered monomer. *J. Biol. Chem.* **287,** 15345–15364

62. Groffen, A. J., Martens, S., Díez Arazola, R., Cornelisse, L. N., Lozovaya, N., de Jong, A. P., Goriounova, N. A., Habets, R. L., Takai, Y., Borst, J. G., Brose, N., McMahon, H. T., and Verhage, M. (2010) Doc2b is a high-affinity Ca2+ sensor for spontaneous neurotransmitter release. *Science* **327,** 1614–1618
63. Hui, E., Johnson, C. P., Yao, J., Dunning, F. M., and Chapman, E. R. (2009) Synaptotagmin-mediated bending of the target membrane is a critical step in Ca(2+)-regulated fusion. *Cell* **138,** 709–721
64. McMahon, H. T., Kozlov, M. M., and Martens, S. (2010) Membrane curvature in synaptic vesicle fusion and beyond. *Cell* **140,** 601–605
65. Di Paolo, G., and De Camilli, P. (2006) Phosphoinositides in cell regulation and membrane dynamics. *Nature* **443,** 651–657
66. Blondeau, F., Ritter, B., Allaire, P. D., Wasiak, S., Girard, M., Hussain, N. K., Angers, A., Legendre-Guillemin, V., Roy, L., Boismenu, D., Kearney, R. E., Bell, A. W., Bergeron, J. J., and McPherson, P. S. (2004) Tandem MS analysis of brain clathrin-coated vesicles reveals their critical involvement in synaptic vesicle recycling. *Proc. Natl. Acad. Sci. U.S.A.* **101,** 3833–3838
67. Ulmer, T. S., and Bax, A. (2005) Comparison of structure and dynamics of micelle-bound human α-synuclein and Parkinson disease variants. *J. Biol. Chem.* **280,** 43179–43187